New Phytologist

Research

Functions of stone cells and oleoresin terpenes in the conifer defense syndrome

Justin G. A. Whitehill[1], Macaire M. S. Yuen[1], Hannah Henderson[1], Lina Madilao[1], Kristina Kshatriya[1], Jennifer Bryan[1,2], Barry Jaquish[3] and Jörg Bohlmann[1,4,5]

[1]Michael Smith Laboratories, University of British Columbia, 301-2185 East Mall, Vancouver, BC V6T 1Z4, Canada; [2]Department of Statistics, University of British Columbia, Vancouver, BC V6T 1Z4, Canada; [3]British Columbia Ministry of Forests, Lands and Natural Resource Operations, Tree Improvement Branch, Kalamalka Forestry Centre, 3401 Reservoir Road, Vernon, BC V1B 2C7, Canada; [4]Department of Botany, University of British Columbia, 6270 University Boulevard, Vancouver, BC V6T 1Z4, Canada; [5]Department of Forest and Conservation Sciences, University of British Columbia, 2424 Main Mall, Vancouver, BC V6T 1Z4, Canada

Author for correspondence:
Jörg Bohlmann
Tel: +1 604 822 0282
Email: bohlmann@msl.ubc.ca

Received: *24 May 2018*
Accepted: *31 August 2018*

New Phytologist (2019) **221:** 1503–1517
doi: 10.1111/nph.15477

Key words: bark beetles, forest health, *Picea sitchensis*, *Pissodes strobi*, plant resistance, plant–insect interaction, sclereid, terpenoid.

Summary

- Conifers depend on complex defense systems against herbivores. Stone cells (SC) and oleoresin are physical and chemical defenses of Sitka spruce that have been separately studied in previous work.
- Weevil oviposit at the tip of the previous year's apical shoot (PYAS). We investigated interactions between weevil larvae and trees in controlled oviposition experiments with resistant (R) and susceptible (S) Sitka spruce. R trees have an abundance of SC in the PYAS cortex. SC are mostly absent in S trees. R trees and S trees also differ in the composition of oleoresin terpenes. Transcriptomes of R and S trees revealed differences in long-term weevil-induced responses.
- Performance of larvae was significantly reduced on R trees compared with S trees under experimental conditions that mimicked natural oviposition behavior at apical shoot tips and may be attributed to the effects of SC. In oviposition experiments designed for larvae to feed below the area of highest SC abundance, larvae showed an unusual feeding behavior and oleoresin appeared to function as the major defense.
- The results support a role for both SC and oleoresin terpenes and possible synergies between these traits in the defense syndrome of weevil-resistant Sitka spruce.

Introduction

The spruce weevil (*Pissoides strobi*) is the most significant pest of Sitka spruce (*Picea sitchensis*) in North America (Alfaro *et al.*, 2002). In the spring, female weevils lay eggs into the cortex of the apical shoot tip of young trees before expansion of the current year's apical shoot (CYAS) (Fig. 1). The developing larvae feed in the cortex in a downwards direction from the tip to the base of the previous year's apical shoot (PYAS) before excavating pupal chip cocoons. Feeding larvae destroy the phloem, cambium and developing xylem of the PYAS, this process disrupts the flow of water and nutrients to the developing CYAS. A single generation of larvae destroys at least 2 yr of apical shoot growth, resulting in stunted and deformed trees that have lost their apical dominance.

Severe weevil infestation has resulted in government policies to halt the planting of Sitka spruce in western Canada (King & Alfaro, 2009), while the species is widely planted in the UK. The spruce weevil also affects reforestation of white spruce (*Picea glauca*) and its hybrid interior spruce (*P. glauca* × *P. engelmannii* × *P. sitchensis*) as well as Norway spruce (*Picea abies*) in other parts of North America. The identification of weevil-resistant spruce genotypes has been a focus of spruce breeding programs (Kiss & Yanchuk, 1991; King & Alfaro, 2009; King *et al.*, 2011).

Conifers resist stem-feeding insects through a combination of several physical and chemical defenses, which may occur constitutively or are induced by insect attack (Kolosova & Bohlmann, 2012). Chemical defenses of conifers against insects include the accumulation of terpenoids and phenolics (Franceschi *et al.*, 2005; Keeling & Bohlmann, 2006; Raffa, 2014). Terpene-rich oleoresin functions as both a physical and a chemical defense. Oleoresin is constitutively produced and accumulates in spruce stems mostly in cortical resin ducts and in radial resin ducts that reach from the cortex into the xylem (Franceschi *et al.*, 2005; Celedon *et al.*, 2017). Additional oleoresin terpene biosynthesis is induced by wounding or insect attack as part of the development of traumatic resin ducts in the cambium and xylem (Franceschi *et al.*, 2000; Martin *et al.*, 2002; Miller *et al.*, 2005; Zulak *et al.*, 2010). Physical defenses of conifers include bark texture and thickness, calcium oxalate crystals, and stone cells (SC, sclereids) (Franceschi *et al.*, 2005; King *et al.*, 2011; Whitehill *et al.*, 2016a,b). The contribution of a specific defense mechanism to insect resistance and possible interactions of different defenses,

Fig. 1 Oviposition and feeding of spruce weevil on Sitka spruce apical shoots. (a) An apical shoot tip with multiple feeding and oviposition holes, an adult female weevil using its rostrum to produce a hole into the cortex, and oleoresin exuding from the puncture. (b) Close-up image of a weevil fecal plug covering an oviposition hole. (c) Close up image of an adult weevil feeding hole. (d, e) Natural oviposition hole containing a single weevil egg beneath the bark along a sterigmatal ridge. (f) Artificial inoculation of a weevil egg into an artificial oviposition chamber.

are difficult to dissect in conifers when genetic mutants are not available. Although terpenes (Hamberger *et al.*, 2011; Nagel *et al.*, 2014) and phenolics (Hammerbacher *et al.*, 2014; Mageroy *et al.*, 2017) have been targeted in spruce with RNAi or overexpression of biosynthetic genes, transgenic approaches are limited to a few lines of white spruce and Norway spruce; and it takes years for transgenic trees to reach an ecologically relevant age to be tested in controlled experiments with stem-feeding insects.

Naturally occurring, contrasting genotypes of weevil-resistant (R) and weevil-susceptible (S) Sitka spruce (King & Alfaro, 2009; King *et al.*, 2011) have previously been explored to identify components of the chemical and physical defense system. Specifically, the clonally propagated Sitka spruce R genotype H898 and the S genotype Q903 were used to describe terpene and SC defenses (Hall *et al.*, 2011; Whitehill *et al.*, 2016a,b). The H898 R genotype originates from an area where Sitka spruce has historically been exposed to the weevil (King *et al.*, 2011), while the Q903 S genotype is from the weevil-free Haida Gwaii Islands (King & Alfaro, 2009; Robert *et al.*, 2010). In choice experiments with R and S trees, adult weevils avoided feeding on R trees (Robert & Bohlmann, 2010). Weevils showed delayed ovary development and reduced reproductive success on R trees in no-choice experiments (Robert & Bohlmann, 2010). Comparison of R and S trees at the metabolome, genome, transcriptome, proteome and biochemical levels found variations within a set of four (+)-3-carene/(−)-sabinene terpene synthase genes that explained phenotypic differences in (+)-3-carene monoterpene levels (Hall *et al.*, 2011; Roach *et al.*, 2014). High levels of (+)-3-carene are associated with weevil resistance (Robert *et al.*, 2010). The R genotype also has a high abundance of SC at the top of the PYAS, which co-localizes with the oviposition site of weevils, while S trees have low abundance of or lack SC at the apical shoot tip (Fig. 2) (Whitehill *et al.*, 2016a). Stone cells have a high predictive power of weevil resistance in Sitka spruce (King *et al.*, 2011). Stone cells are hypothesized to be a durable quantitative defense that provides resistance to several spruce species against bark beetles and weevils (Wainhouse *et al.*, 1990; King *et al.*, 2011; Whitehill *et al.*, 2016a,b). Experiments with weevils on an artificial diet showed that SC function as a feeding barrier against larvae, disrupting their establishment, development and survival (Whitehill *et al.*, 2016a,b).

In the present study we first validated our previous observations of SC affecting weevil performance gleaned from *in vitro* studies with artificial diets (Whitehill *et al.*, 2016b) by using a set of newly designed *in planta* oviposition experiments. Based on some unexpected results, we then assessed the hypothesis that SC may interact with other components of the Sitka spruce defense system, specifically terpene oleoresin. In addition, given that developing weevil larvae spend several weeks feeding in the cortex of the host tree, we tested the transcriptome of R and S trees for possible long-lasting changes that were indicative of additional defenses.

Materials and Methods

Plants

Origins and growing conditions of clonally propagated Sitka spruce R and S genotypes were described previously (Robert & Bohlmann, 2010; Whitehill *et al.*, 2016a,b). In brief, the R genotype H898 is from the low elevation mainland of British Columbia, Canada (49°14′N; 122°36′W). The S genotype Q903 is from the Haida Gwaii Islands (53°55′N; 132°05′W). Grafted saplings of R and S trees were produced in 2008. Plants were maintained year round in 1-gallon pots in a nursery located outside on the University of British Columbia Vancouver campus (49°15′40.82″N; 123°15′09.89″W), British Columbia, Canada.

Insects

Weevil eggs were isolated from apical shoots of naturally attacked trees at the Kalamalka Research Station in Vernon, British Columbia, Canada (50°16′00″N; 119°16′18″W). Infested apical shoots were collected 6 May 2013 (276 growing degree days (GDD, Whitehill *et al.* (2016b)) and 26 April 2016 (310 GDD). Cut ends were sealed with paraffin and stored at 4°C until eggs were isolated as described in Whitehill *et al.* (2016b) within the following 6 wk. Eggs were viable in stored apical shoots for up to 3 months. Apical shoots contained 88.3 ± 1.7 eggs ($n = 10$ in 2013) and 48.2 ± 9.0 eggs ($n = 17$ in 2016) at the time of isolation. Eggs were used separately based on origin, such that each group of eggs originating from a single shoot represented a separate cohort. Eggs were stored for a maximum of 3 d in sterile MilliQ H_2O at 4°C before experiments took place.

Experimental design to assess weevil performance on R and S trees

Controlled inoculation experiments with R and S trees were performed to coincide with the natural phenological window of oviposition based on GDDs. Growing degree days were calculated from daily maximum and minimum temperatures measured in Vancouver (http://climate.weather.gc.ca).

Expt I: Artificial oviposition chamber and egg inoculations at 0–2 cm from the tip of the PYAS Twelve R and 12 S trees were used. Treatments started on 20 May 2013 (465 GDD) and concluded 2 July 2013 (923 GDD). Trees were organized as a

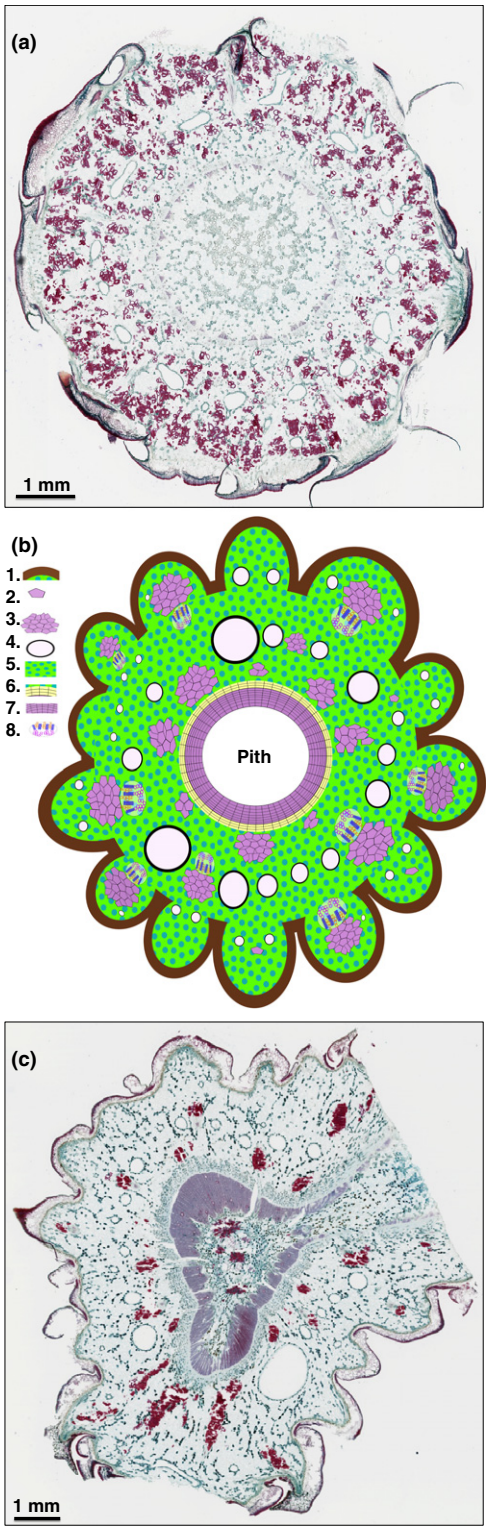

Fig. 2 Defensive structures in the cortex of Sitka spruce resistant (R) and susceptible (S) trees. (a) Cross-section at SC (stone cell) zone in the top 0–2 cm of the previous year apical shoot (PYAS) tip of an R tree. Abundant SC in the cortex are stained purple with phloroglucinol–HCl. (b) Schematic of major anatomical features of the apical shoot cross-section: 1, outer bark; 2, single SC; 3, SC cluster; 4, cortical resin duct; 5, polyphenolic cells; 6, phloem; 7, xylem; 8, needle fascicular bundle. (c) Cross-section in the top 0–2 cm of the PYAS tip of an S tree. Low abundance of SC appear as purple clusters in the cortex stained with phloroglucinol–HCl.

randomized complete block with three treatment groups. Each treatment group consisted of four R and four S trees. Treatments applied to PYAS were control (treatment 1), artificial oviposition chamber (AOC, treatment 2), and AOC plus weevil eggs (treatment 3). Previous year's apical shoots of R trees were 41.3 ± 1.6 cm (SEM) in length; S tree PYAS were 39.7 ± 1.1 cm (SEM). Treatments were applied to the top 2 cm of PYAS, the site of natural oviposition and the point of highest SC abundance in R trees (Whitehill *et al.*, 2016a). A Dremel® with 1 mm drill bit was used to excavate 20 AOC in the cortex of the PYAS of each tree for treatments 2 and 3, and were placed below the base of needles in the middle of sterigmata on the outer bark to emulate natural oviposition sites (Fig. 1). In treatment 3, 10 AOC with no sign of resin flooding were selected for each tree on 21 May 2013 (472 GDD) and inoculated with a single egg per AOC using 80 eggs from a single cohort. The top 2 cm of the PYAS of all trees in treatments 1–3 were wrapped with Parafilm. Trees were kept under natural conditions outside on the University of British Columbia campus. An additional four R and four S trees received treatment 3 and one R and one S tree was dissected every 2 wk for 6 wk to follow weevil development. Weevils had entered the final stage of larval development in S trees on 2 July 2013 (923 GDD), which was set as the date to collect plant and insect samples.

Expt II: Artificial oviposition chamber and egg inoculations at 4–6 cm from the tip of the PYAS Sixteen R and 16 S trees were used in the experiment in a randomized complete block following the general design of Expt I with two modifications. First, treatments were applied 4–6 cm below the CYAS and PYAS boundary beneath the area of high SC abundance in R trees (Whitehill *et al.*, 2016a). Second, weevils were applied to trees as neonate larvae reared on semi-artificial diet for 3 d as described in Whitehill *et al.* (2016b) with or without antibiotics (0.04% w/w tetracycline; Sigma) (Supporting Information Methods S1). Treatments were control (treatment 1), AOC (treatment 2), AOC plus neonate larvae reared on diet without antibiotic (treatment 3), and AOC plus neonate larvae reared on diet with antibiotic (treatment 4). All treatments were applied 5 May 2016 (500 GDD). The experiment ended on 21 June 2016 (929 GDD) to reproduce the GDD accumulation in Expt I. As treatments 3 and 4 did not yield any statistically significant differences for the variables analyzed, data from these two treatments were pooled into a single treatment group.

Collection of bark and weevil larvae from Expts I and II

Spruce bark and weevil larvae were collected on 2 July 2013 (923 GDD – Expt I) and 21 June 2016 (929 GDD – Expt II). Bark samples (including outer bark, cortex, phloem, cambium, and traces of outer xylem) were used for terpene and transcriptome analyses. Four biological replicates were analyzed for each genotype and treatment. Bark from the top 0–2 cm (Expt I) or 4–6 cm (Expt II) of the PYAS bark was sampled from trees in treatment 1 and treatment 2, frozen in liquid N_2 and stored at −80°C. Bark from trees in treatment 3 in Expt I and treatments 3 and 4 in Expt II were harvested by removing outer bark tissues starting at the site of inoculation to access larval feeding galleries. Individual galleries were then dissected using a scalpel and forceps (Rubis, Switzerland). The outer bark covering galleries was removed until a larvae or chip cocoon was found. Larvae and pupae were removed from galleries, placed into 0.2 ml polymerase chain reaction (PCR) tubes and immediately processed as described in Whitehill *et al.* (2016b). Length of galleries was recorded. The cortex surrounding the galleries was collected from the lower 2 cm of a larvae gallery and included a 1 cm border of bark tissue adjacent to and including the larval feeding margin after removal of the insect and frass, for metabolite and transcript analyses (Fig. 1). Tissues from galleries of an individual tree were pooled and treated as a single biological replicate. Frass was collected from each gallery and also pooled within tree. Gallery bark and weevil frass were immediately frozen in liquid N_2 and stored at −80°C until further analyses.

Assessment of weevil performance

The number and fresh weight of larvae and pupae recovered from each tree in Expts I and II was recorded. Mandibles, digestive tracts, growth and development of weevils, as well as the presence of SC in frass were evaluated as described in Whitehill *et al.* (2016b). Larvae growth and mandible wear were compared between R and S genotypes using analysis of variance (ANOVA). Exploratory analyses of data and Levene's test were used to evaluate normality and equality of variance. When data did not pass normality requirements for ANOVA analysis, square root, logarithmic, and arctan transformations were used. Following significant *F*-tests, means were separated post hoc using the least significant difference (LSD) test ($\alpha = 0.05$). For data outcomes that did not meet assumptions of normality and homogeneity of variance, nonparametric methods were used. Variables were rank-transformed and analysed using the Kruskal–Wallis test to identify significant differences between genotypes. The Kruskal–Wallis test was also used post hoc to separate genotype differences in pairwise comparisons ($\alpha = 0.05$). All data were analyzed using IBM SPSS Statistics v.19 (SPSS Inc., Chicago, IL, USA).

Microscopy and imaging

Details of microscopy and imaging are described in Methods S1. In general, spruce PYAS samples from the top 2 cm (Fig. 2) and weevil frass samples were processed and imaged as described in Whitehill *et al.* (2016a).

Terpene analysis

Terpenes in samples from Expts I and II were extracted and analyzed by gas chromatography (GC) as described in Robert *et al.* (2010) with four biological replicates for each treatment and genotype. Details of the monoterpene and diterpene analyses are described in Methods S1. All quantitative terpene data were analyzed using IBM SPSS Statistics v.19. Due to limited quantities of R frass tissues from Expt I, a single pooled monoterpene extract (consisting of frass from four biological replicates) was analyzed for comparative purposes.

Transcriptome analysis

Transcriptomes were analyzed for PYAS bark samples of Expt I with four biological replicates for each treatment (1–3) and genotype (R and S). Bark samples were ground to a fine powder and total RNA extracted using the Purelink® Plant RNA Reagent (Life Technologies, Carlsbad, CA, USA). RNA concentration was determined using a NanoDrop 1000 (Thermo Scientific, Waltham, MA, USA). RNA integrity (RIN) was assessed using Bioanalyzer 2100 RNA Nano chip assays (Agilent, Santa Clara, CA, USA). The minimum RIN was 8.0. cDNA library construction and transcriptome sequencing was performed at the McGill University and Génome Québec Innovation Centre to generate 24 libraries (two genotypes, three treatments, four replicates) of 100-bp, paired-end (PE) strand-specific Illumina HiSeq reads. Sequence data are available at NCBI (accession no. PRJNA398042). Sequence quality was assessed using FastQC (Andrews, 2010). Adapter sequences were trimmed with TRIMMOMATIC (v.0.30) (Bolger *et al.*, 2014). BBMerge from the BBMap software suite (v.35.92) (Bushnell, 2017) was used with the 'verystrict' setting to merge overlapping paired end (PE) reads to generate single ended reads to improve the contiguity of the assembly. Merged and unmerged reads from all 24 libraries were pooled to generate a *de novo* transcriptome assembly using TRINITY (v.2.20) with option 'min_kmer_cov = 4' (Grabherr *et al.*, 2011). The assembly was rendered nonredundant using CD-HIT-EST (v.4.6.1) (Fu *et al.*, 2012). TransDecoder (Haas *et al.*, 2013) was used to generate the predicted peptides in the assembly. Contigs with annotation to fungal, bacterial and ribosomal sequences with a BLAST parameter of 95% nucleotide identity and 90% amino acid coverage were removed before differential expression (DE) analyses. Differential expression analysis was performed on contigs with expression of at least 1 count per million (cpm) in not < 2 libraries using the voom/limma (Law *et al.*, 2014) package in R with quantification results generated with SAILFISH (v.0.6.3) (Patro *et al.*, 2014) set to default parameters. All statistically significant (adjusted P-value ≤ 0.05) DE contigs with an absolute $\log_2$ fold change ≥ 2 were annotated with BLASTX against the NCBI NR database with *e*-value cutoff at 1e-10. Genotype and treatment comparisons were performed to identify DE contigs. Heatmaps were generated that focus on DE contigs for two pairwise comparisons using the D3HEATMAP package (Cheng, 2016) from R (R Core Team, 2013). Volcano plots of overall DE patterns among comparison groups were generated using ggplot2. Codes for DE analyses and for the generation of figures are available on GitHub (https://github.com/myuen/White_Pine_Weevil_DE).

Results

Larvae performance in R and S trees

The overall objective of this study was to elucidate mechanisms by which R trees resist weevils, starting out by validating effects of SC *in planta* following the previous observation of their effects in *in vitro* experiments (Whitehill *et al.*, 2016b). In Expt I, trees were inoculated with weevil eggs at the top of the PYAS emulating natural oviposition behavior (Fig. S1). In this experiment, larvae performed better on S trees than on R trees (Fig. 3). A lower proportion of larvae survived on R trees than on S trees. Head capsules of larvae recovered from R trees were about half the size of those from S trees ($F_{1,20} = 37.311$; $P < 0.001$). Development of six of the seven larvae recovered from R trees was arrested in the 1st ($N = 2$) or 3rd ($N = 4$) instar, while larvae recovered from S trees had developed to the 4th instar ($N = 14$) or formed pupae ($N = 4$). Larvae from R trees weighed less ($F_{1,23} = 24.826$; $P < 0.001$) than those from S trees. Only one pupa was recovered from an R tree, which was smaller (12.5 mg) than the pupae (19.0 mg ± 0.69 mg) isolated from S trees. Gallery length was measured as an indicator of feeding activity. Galleries of larvae on R trees were significantly shorter ($F_{1,20} = 33.150$; $P = 0.002$) than galleries in S trees. All gallery start sites were within the 0–2 cm region where eggs were placed with a typical downwards direction of gallery formation.

The *in planta* performance of larvae in Expt I confirmed the observation of effects of SC on the development of larvae in *in vitro* studies that used artificial diet supplemented with SC (Whitehill *et al.*, 2016b). We therefore hypothesized that larvae would perform better on R trees in Expt II, in which trees were inoculated below the SC zone of the PYAS. Surprisingly, larvae showed a different feeding behavior in this experiment. Both in the R and in the S trees, larvae formed feeding galleries by moving upwards, as opposed to their natural downwards movement. This feeding behavior was observed with all larvae on the R trees and with all but two larvae on the S trees. Galleries were only about half the length in Expt II compared with galleries formed in Expt I (Fig. 3), and larvae did not reach the SC zone in the R trees. Survival of larvae appeared to be lower in Expt II than in Expt I. Larvae did not progress through as many developmental stages, and they were generally smaller in Expt II. As in Expt I, the proportion of larvae surviving on R trees in Expt II was lower than on S trees. Head capsules of larvae ($H = 9.600$, $P = 0.002$; $N = 12$) recovered from R trees were about half the size of larvae from S trees. Only four larvae were recovered from R trees and all were arrested in the 1st instar of development. Eight larvae were recovered from S trees, and their development was restricted to the 1st ($N = 4$) and 2nd ($N = 4$) instars. Only two insects recovered from S trees had developed into pupae. Weight of larvae isolated from R and S trees differed ($H = 10.604$, $P < 0.001$; $N = 14$), with larvae isolated from R trees being very small compared with S tree larvae. Gallery length was shorter in R trees ($H = 10.588$, $P < 0.001$; $N = 14$) than S trees.

The results from Expt II were unexpected, as larvae were strongly differentially affected on R and S trees, despite their inoculation and development in a section of the PYAS away from the SC zone. This result suggested that other defense mechanisms affected larvae on R trees in Expt II, and, by extension, additional defenses may have acted in combination with SC in R trees in Expt I.

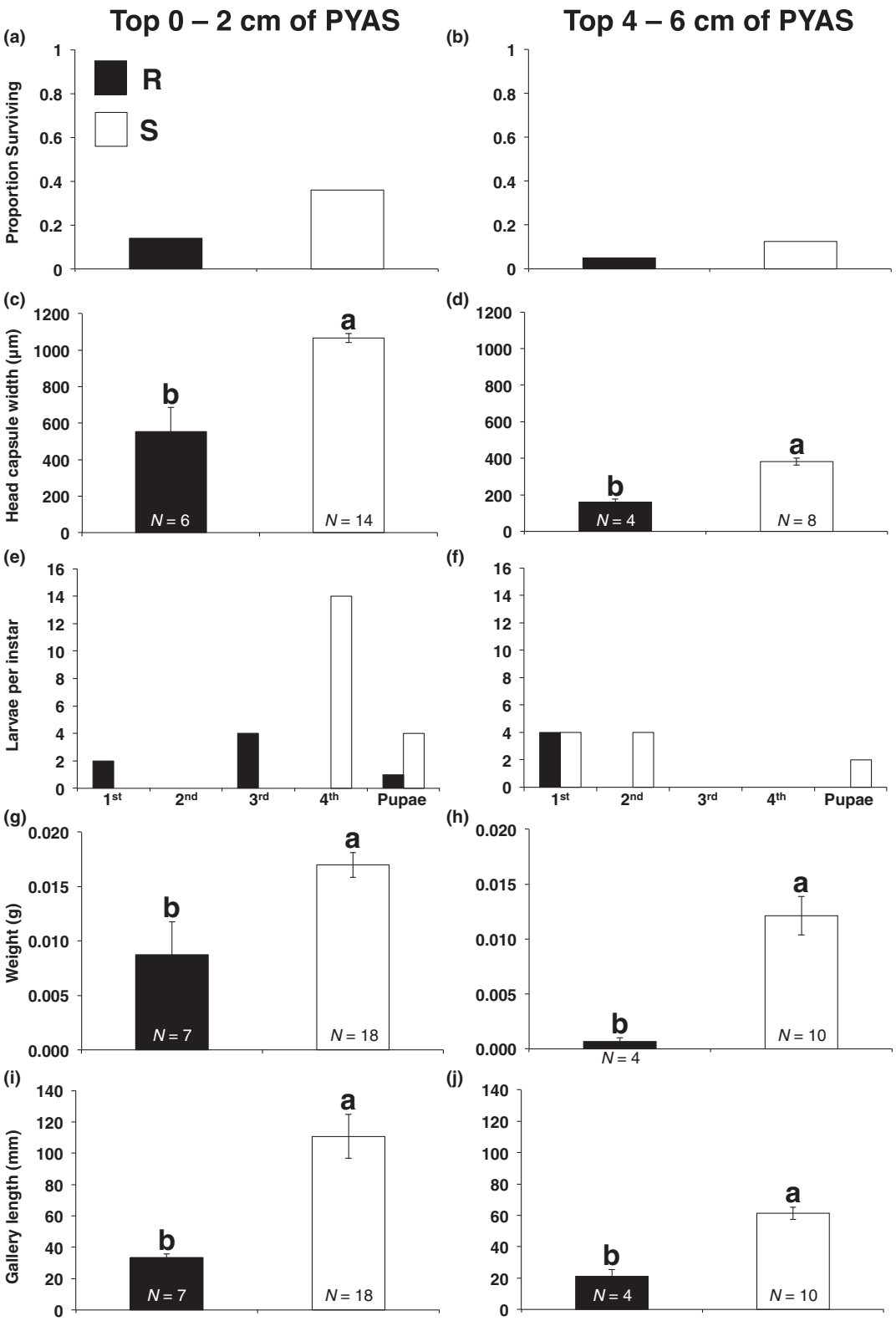

Fig. 3 Performance of weevil larvae in Expts I and II. (a, c, e, g, i) Results from inoculations on resistant (R) and susceptible (S) Sitka spruce trees at the top 0–2 cm of the previous year apical shoot (PYAS). (b, d, f, h, j) Results from inoculations on R and S trees at 4–6 cm below the tip of the PYAS. (a, b) Proportion of larvae surviving at the end of Expt I ($N = 40$) and Expt II ($N = 80$). (c, d) Average head capsule widths (in µm) of larvae recovered from R and S trees at the end of experiments. (e, f) Distribution of larval instars recovered at the end of experiments. (g, h) Average larval weights (g) at the end of experiments. (i, j) Average gallery lengths (mm) of weevil larvae re-isolated at the end of experiments. Error bars represent ± SE of the mean. Weevil performance on R and S trees was analyzed using one-way analysis of variance (ANOVA). Different letters indicate significantly different means separated post hoc following significant *F*-tests by the protected LSD test ($\alpha = 0.05$).

Effects of R and S trees on mandible wear and digestive tract

To complete the characterization of larval performance *in planta* on R and S trees, we also assessed mandible wear and effects on the digestive tract, as was previously carried out in the artificial diet study (Whitehill *et al.*, 2016b). Overall, larvae from R and S trees in Expt I had more mandible wear than larvae isolated from R and S trees in Expt II (Fig. 4). In Expt I, mandible wear did not differ ($F_{1,16} = 2.151$; $P = 0.166$) between larvae isolated from R ($N = 6$) and S ($N = 14$) trees, when all larvae were considered. However, larvae ($N = 2$) recovered from R trees that were arrested in the 1st instar in the SC zone had substantial mandible damage. Larvae that had formed galleries past the SC zone in R trees and progressed to the 3rd instar ($N = 4$) had no quantifiable signs of mandible damage. Larvae from S trees in Expt I were in the 4th instar and showed mandible damage. In Expt II, mandible wear differed between the R and S genotypes ($F_{1,9} = 7.349$; $P = 0.030$) with larvae feeding in S trees having more mandible wear. These results confirmed that possible effects of SC on mandible wear may be confounded by the overall progression of larval development (Whitehill *et al.*, 2016b), as larvae renew their mandibles during molting.

In Expt I, intact SC were found in frass of larvae ($N = 3$) recovered from R trees, but no SC were observed in larvae ($N = 4$) frass on S trees (Fig. S1). The morphology of gut bacteriomes differed between larvae recovered from R and S trees (Fig. S2). Bacteriomes in larvae ($N = 3$) recovered from R trees appeared deflated or curled and smaller compared with larvae ($N = 6$) from S trees. These results confirm observations from the *in vitro* feeding assays on an SC-enriched artificial diet (Whitehill *et al.*, 2016b). In Expt II, larvae were completely encased in oleoresin and could not be dissected for microscopy.

Total monoterpene accumulation in R and S trees and differential exposure of larvae to monoterpenes

The results of Expt II suggested that other defense mechanisms, in addition to SC, affected the performance of larvae on R trees. One important observation was that galleries on R trees in Expt I as well as galleries in R and S trees in Expt II were flooded with oleoresin, and larvae were heavily incrusted with oleoresin (Fig. 5). In contrast, larvae in galleries on S trees in Expt I were not exposed to a similar amount of oleoresin in feeding galleries. These observations suggested that oleoresin volume or composition may have differentially affected larvae on R and S trees within Expt I and between Expts I and II. We therefore performed quantitative and qualitative analyses of oleoresin monoterpenes and diterpenes in bark samples from the two

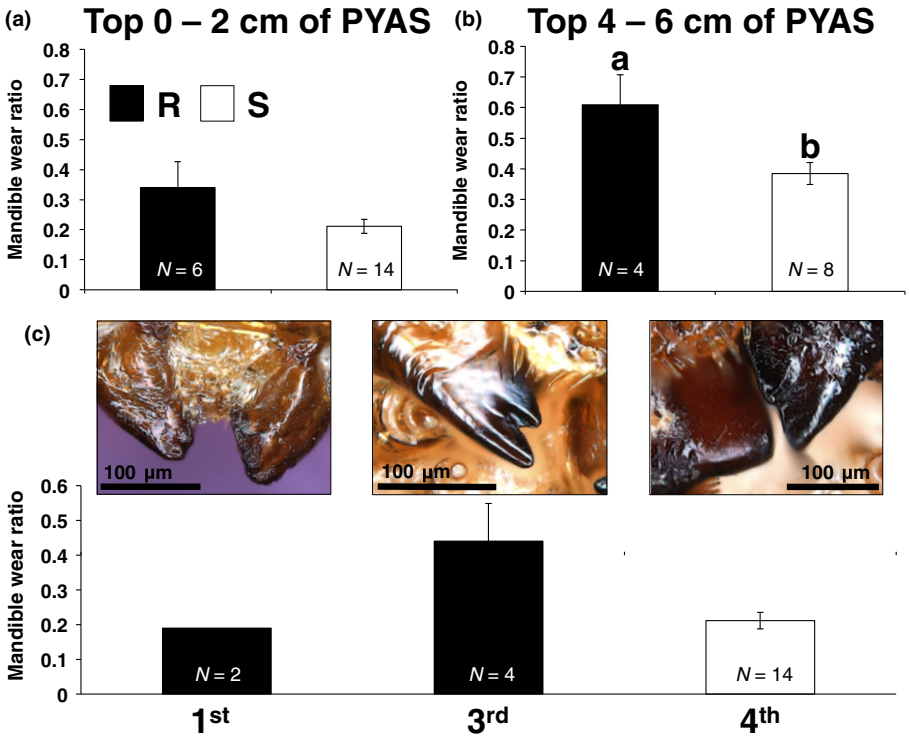

Fig. 4 Mandible wear of larvae feeding on resistant (R) and susceptible (S) Sitka spruce trees. Mandible wear was measured as in Whitehill *et al.* (2016b), where greater mandible wear is indicated by a smaller ratio. (a) Expt I, mandible wear for all larvae recovered from R trees or S trees at the end of the experiment. (b) Expt II, mandible wear for all larvae recovered from R trees or S trees at the end of the experiment. (c) Expt I, mandible wear images and ratios for larvae at different stages of development at the end of the experiment: 1st instar larvae that were arrested in the stone cell (SC) zone on R trees; 3rd instar larvae that had passed the SC zone, molted, and produced new mandibles on R trees; 4th instar larvae from S trees, whose mandibles may have been affected by excavation of pupal chip cocoons in the lignified xylem. Error bars represent ± SE of the mean. Mandible wear was assessed and differences between R and S trees were analyzed using one-way analysis of variance (ANOVA). Different letters indicate significantly different means separated post hoc following significant *F*-tests by the protected LSD test ($\alpha = 0.05$). PYAS, previous year apical shoot.

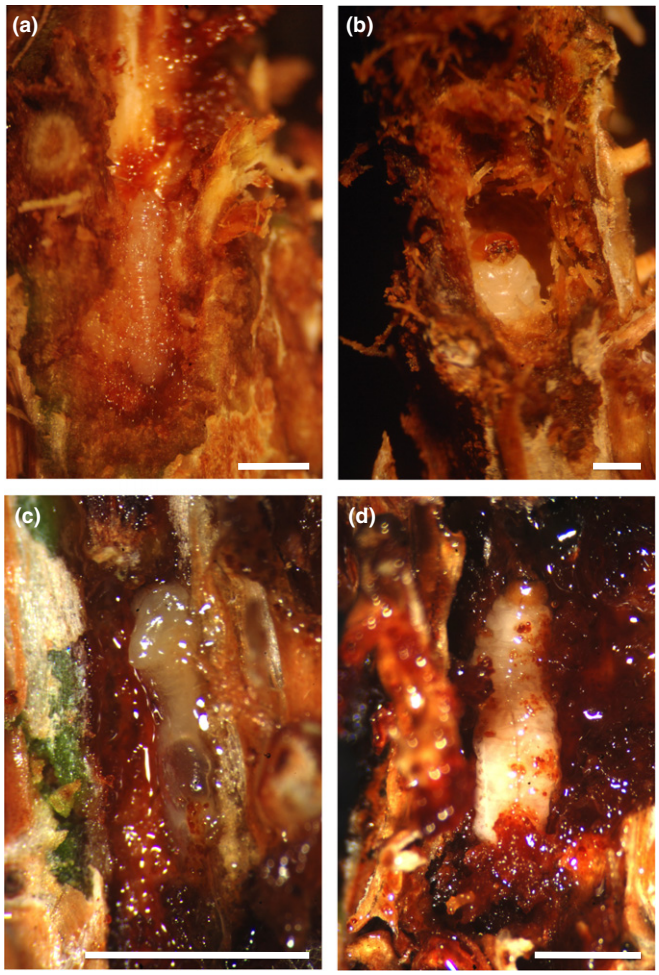

Fig. 5 Representative feeding galleries with weevil larvae on resistant (R) and susceptible (S) trees at the end of Expts I and II. (a) 3rd instar larva incrusted in oleoresin feeding in downward direction in R tree cortex in Expt I. (b) 4th instar, prepupal larva forming chip cocoon (pupal chamber) after feeding in downward direction in S tree cortex in Expt I. (c) 1st instar larva flooded in oleoresin while attempting to feed in upward direction in R tree cortex in Expt II. Oleoresin bubble is visible through the outer cuticle in the digestive tract of the insect, likely caused by ingestion of pure terpene oleoresin. (d) 2nd instar larva incrusted in terpenes feeding in upward direction in S trees cortex in Expt II. Bars, 1 mm.

experiments (Fig. 6). We also measured terpenes in weevil frass as an indicator of the exposure of feeding larvae to oleoresin.

In Expts I and II, the total amount of monoterpenes did not differ between R and S trees (Expt I: $F_{1,23} = 0.128$, $P = 0.725$; Exp. II: $F_{1,44} = 0.040$; $P = 0.843$) and no interaction was observed for tree genotype × treatment (Expt I: $F_{5,23} = 0.552$, $P = 0.587$; Expt II: $F_{7,44} = 1.593$, $P = 0.209$). In Expt I, there were significant differences for total monoterpenes between treatments 1, 2, and 3 ($F_{2,23} = 7.886$, $P = 0.005$) with samples from gallery tissues (treatment 3) having higher concentrations of total monoterpenes than samples from controls (treatment 1) (Fig. 6a). These samples did not contain obvious traces of insects or frass. Strikingly, we found that monoterpenes accumulated in frass produced by larvae feeding on R trees, while frass from larvae that fed on S trees had low levels of monoterpenes (Fig. 6a), supporting the observation from visual inspection of galleries that larvae in Expt I on R trees were substantially more exposed to oleoresin than larvae on S trees (Fig. 5a,b). In Expt II, there were also highly significant differences for total amounts of monoterpenes between treatments 1, 2, 3 and 4 and frass ($F_{3,44} = 97.865$; $P < 0.001$) (Fig. 6b). Weevil frass contained, by far, the highest quantities, followed by gallery (treatments 3 and 4), and AOC (treatment 2) and control (treatment 1) samples. As a major contrast with Expt I, total monoterpenes accumulated to extremely high quantities in frass of larvae on both R and S trees in Expt II. Total monoterpenes were significantly more abundant in larvae frass from both genotypes when compared with gallery (R = 14.0-fold and S = 14.1-fold higher), AOC (R = 19.6-fold and S = 26.3-fold higher), and control (R = 15.8-fold and S = 37.1-fold higher) tissues. This result showed that larvae were heavily exposed to oleoresin monoterpenes on R and S trees in Expt II, on R trees in Expt I, but not on S trees in Expt I.

Oleoresin monoterpene composition

In Expts I and II, abundance of most individual monoterpenes showed similar patterns to that of total monoterpenes (Fig. S3). Nine different monoterpenes ((-)-α-pinene, (-)-camphene, (+)-β-pinene, (+)-sabinene, (+)-3-carene, myrcene, (−)-limonene, (−)-β-phellandrene, and terpinolene) were detected in samples from Expt I. All nine monoterpenes were present in the R tree samples and, except for (+)-3-carene, were also present in S tree samples. All monoterpenes were present in the highest quantities in the frass of larvae on R trees, but were very low or absent in frass of larvae on S trees. In samples from Expt II, we identified four additional monoterpenes, namely α-thujene, (−)-α-phellandrene, α-terpinene and γ-terpinene (Fig. S4). All 13 compounds were detected in both genotypes. α-Thujene was only found in S tree galleries and frass but not in control or AOC treatments. Only traces of (+)-3-carene were detected in S tree samples. Unlike in Expt I, in which only frass from larvae on R tress was highly enriched for all individual monoterpenes, in Expt II most monoterpenes were highly enriched in frass of larvae from both R and S trees (Figs S3, S4). Quantities of the monoterpenes (−)-α-pinene, (+)-β-pinene, terpinolene, α-terpinene and γ-terpinene did not differ in frass between genotypes. Several compounds were significantly more abundant in the frass of S tree larvae including (−)-camphene, myrcene, (−)-limonene, (−)-β-phellandrene and (−)-α-phellandrene. Three monoterpenes were significantly more abundant in frass from larvae on R trees (+)-sabinene, (+)-3-carene, and α-thujene. Notably, the amounts of (+)-3-carene and (+)-sabinene were, respectively, 30-fold and 10-fold higher in frass from larvae on R trees compared with S trees.

Diterpene accumulation in R and S trees and differential exposure of larvae to diterpenes

Patterns of diterpene accumulation followed the same patterns as observed for monoterpene accumulation in Expts I and II (Fig. 6). The total amount of diterpenes did not differ between R and S trees (Expt I: $F_{1,31} = 2.603$; $P = 0.210$; Expt II:

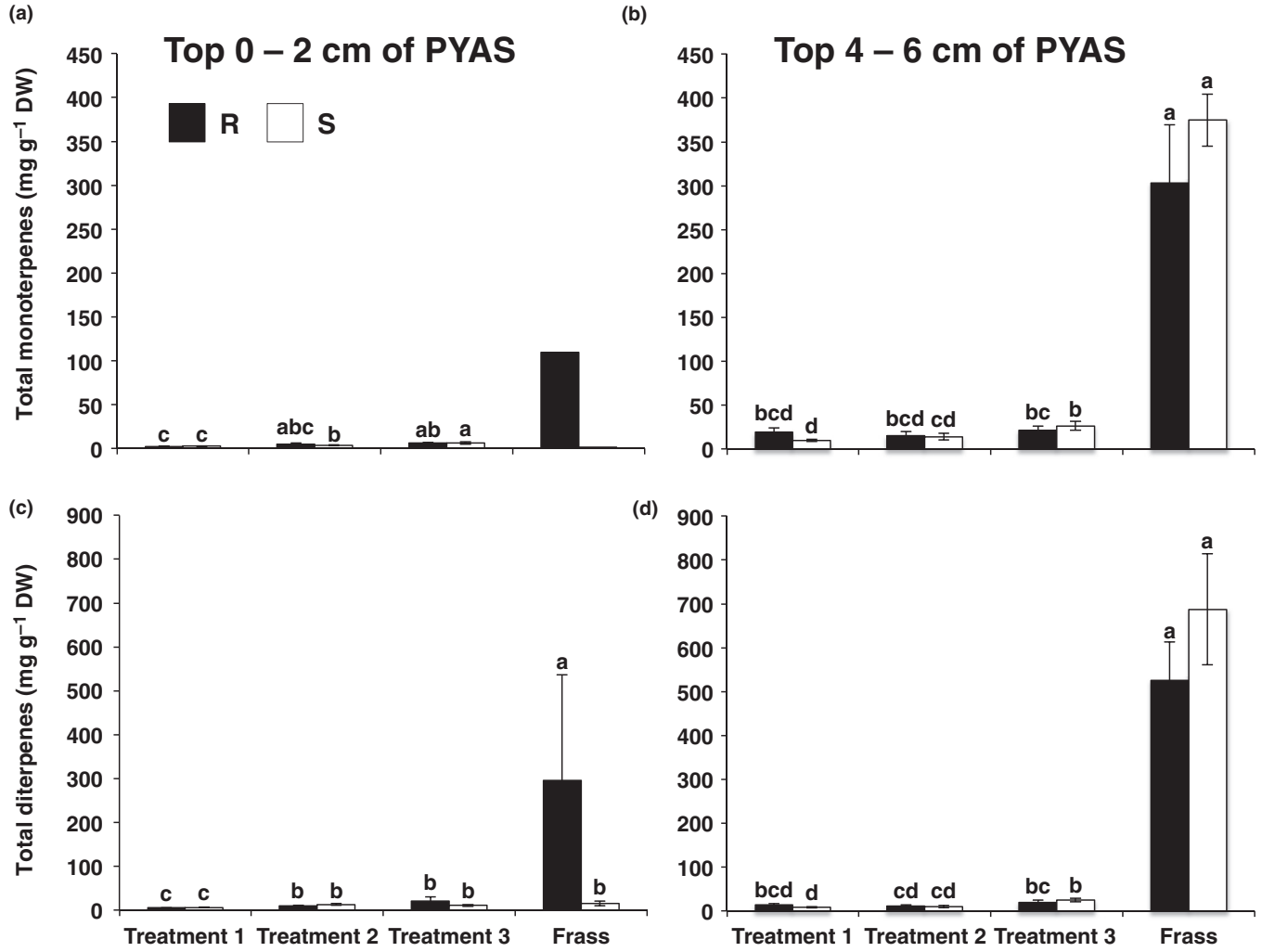

Fig. 6 Monoterpene and diterpene levels in cortex tissues and weevil frass. (a, c) Results from Expt I. (b, d) Results from Expt II. (a, b) Total monoterpenes and (c, d) total diterpenes in cortex of resistant (R) and susceptible (S) trees from controls (treatment 1), tissue surrounding artificial oviposition chambers (AOC, treatment 2), tissue surrounding insect galleries (treatment 3), and in weevil frass. Quantities are presented as mg g^{-1} DW. Error bars represent ± SE of the mean. Differences between genotype and treatment were analyzed using two-way analysis of variance (ANOVA). Different letters indicate significantly different means separated post hoc following significant *F*-tests by the protected LSD test ($\alpha = 0.05$). PYAS, previous year apical shoot.

$F_{1,44} = 0.007$; $P = 0.934$) and no interaction was observed for tree genotype x treatment (Expt I: $F_{7,31} = 2.305$; $P = 0.102$; Expt II: $F_{7,44} = 1.424$; $P = 0.253$) in Expts I and II. In Expts I and II, the total quantity of diterpenes differed between treatments and frass (Expt I: $F_{3,31} = 3.105$, $P = 0.045$; Expt II: $F_{3,44} = 129.159$, $P < 0.001$) with samples from galleries (treatment 3 in Expt I, treatments 3 and 4 in Expt II) and AOC (treatment 2) having higher levels of diterpenes than control samples (treatment 1) (Fig. 6c,d). As with monoterpenes, we also discovered a striking contrast for total diterpene accumulation in frass between Expts I and II (Fig. 6c,d). High quantities of diterpenes were found in frass of larvae on R trees in Expt I, while in Expt II diterpenes were highly accumulated in frass of larvae on both R and S trees.

Oleoresin diterpene composition

In Expt I, individual diterpene quantities followed the overall trends observed for total diterpenes with only a few compounds differing by genotype and treatment (Table S1). Overall, frass from larvae on R trees contained the statistically highest quantities of each individual diterpene compound, except for pimaradiene which was more abundant in S tree gallery tissues. Notably, the quantity of dehydroabietic acid was 52.3, 22.2 and 16.0 fold higher in frass of larvae on R trees, compared with control (treatment 1), AOC (treatment 2), and gallery tissues (treatment 3), respectively. Compared with frass of larvae on S trees, dehydroabietic acid was 7.9 fold higher. Dehydroabietic acid was previously associated with weevil resistance (Robert *et al.*, 2010). In Expt II, quantities of individual diterpenes also followed similar trends as totals (Table S2). However, the diversity of diterpenoids detected was less than in Expt I. The major diterpenes found in samples from Expt II were comprised mainly of diterpene resin acids. Notably, the only diterpene more abundant in frass of larvae on R trees, compared with frass of larvae on S trees, was dehydroabietic acid.

Differential transcriptome responses in R and S trees

Given that factors in addition to SC appear to contribute to defense in R trees in Expt I, we assessed the transcriptome response of R and S trees affected by the different treatments (Fig. 7). Weevil larvae spend several weeks feeding in the cortex of the PYAS. We therefore selected a time point 50 d after inoculation that coincided with larvae completing their life cycle on S trees to assess the components of the transcriptome response that may stay up- or downregulated throughout the time that trees are exposed to weevils. The transcriptome assembly (Table S3) and the analysis for DE covered 24 individual transcriptomes (two genotypes, three treatments, four biological replicates).

Principal component analysis (PCA) of variation among transcriptomes revealed a reproducible (replicates generally grouped together) separation between genotype and treatments (Fig. 7a). Transcriptome differences separated the R and S genotypes in the first principal component (PC1). The second principal component (PC2) separated treatments within the S genotype with no impact to the R genotype. Transcriptomes generated from control and AOC-treated S trees co-localized in the PCA grid. Gallery transcriptomes from S trees localized as a separate group. Principal component 1 and PC2 did not yield discernible differences between treatments for the R trees. Overall, PC1 and PC2 combined accounted for 55% of the original variance, with 37.9-% explained by PC1 and 17.1% explained by PC2. PCA patterns revealed differences between transcriptomes of R and S trees with substantial changes affected by larvae in the S trees.

Transcriptomes from control trees revealed constitutive differences with 4475 contigs (i.e. transcripts) DE between the R and S genotypes (Table S4). Of these transcripts, 2257 were more abundant ($\log_2$ fold change > 2; $\alpha = 0.05$) in the R genotype and 2218 were more abundant in the S genotype (Fig. 7b,c). Using annotations of defense genes in the white spruce genome as a reference (Warren *et al.*, 2015) we identified 21 constitutively DE transcripts as putatively involved in defense (Table S5). Hierarchical clustering analysis (HCA) of these 21 transcripts revealed a clear separation of two main clusters separated by higher expression in constitutive R trees (9 transcripts) or S trees (12 transcripts) (Figs 7e, S5). The 21 transcripts belonged to the cytochrome P450 gene family (12 transcripts; seven with higher abundance in the R genotype, and five with higher abundance in the S genotype), the phenylpropanoid pathway (six transcripts; two with higher abundance in the R genotype, and four with higher in the S genotype), the 2-*C*-methyl-D-erythritol 4-phosphate (MEP) pathway (one transcript with higher abundance in the S genotype), the flavonoid pathway (one transcript with higher abundance in the S genotype), and the mevalonate pathway (MEV) (one transcript with higher abundance in the S genotype) (Figs 7e, S5; Table S5).

The effect of larvae on transcripts that were DE as part of a long-term response to AOC or weevils was evaluated separately for each genotype (Fig. 7b,d). In R trees, no transcripts were DE between control and AOC or between AOC and gallery tissues at the 50-d time point (Fig. 7b). Control vs gallery tissues identified only three DE contigs (two upregulated; one downregulated), none of which had informative annotations (Table S6). In contrast, a much stronger response was observed in the gallery tissues of S trees (Fig. 7b). In S trees, 7178 transcripts were DE between controls and gallery tissues, with 3325 transcripts more abundant ($\log_2$ fold change > 2; $\alpha \leq 0.05$) in galleries and 3853 more abundant in controls (Fig. 6b; Table S7). In total, 5712 transcripts were DE between S tree AOC and gallery tissues, with 2022 more abundant in galleries and 3690 more abundant in the AOC site tissues (Fig. 7b, d; Table S8). Of these 5712 transcripts, 41 (25 upregulated and 16 downregulated in galleries of the S genotype) matched with previous annotations as defense genes in the white spruce genome (Warren *et al.*, 2015) (Table S5). HCA of these genes revealed a clear separation between genotype and treatment groups (Figs 7f, S6). Control and AOC samples clustered together while galleries separated in both genotypes, however S galleries separated from all other comparisons with the other treatments and genotypes having a similar expression profile. Transcripts clustered into two main groups, either upregulated (25 transcripts) or downregulated (16 transcripts) by weevil feeding in S trees (Fig. 7f; Table S9). These transcripts belonged to cytochromes P450 (21 transcripts; nine upregulated and 12 downregulated in galleries of the S genotype), the phenylpropanoid pathway (seven transcripts; six up-regulated and one down-regulated in galleries of the S genotype), the MEP pathway (one downregulated in galleries of the S genotype), the flavonoid pathway (nine transcripts; eight upregulated and one downregulated in galleries of the S genotype), the MEV pathway (one upregulated in galleries of the S genotype), and terpenoid biosynthesis (two transcripts; one upregulated and one downregulated galleries of the S genotype) pathways (Figs 7f, S6; Table S9). Only a single transcript was DE (downregulated) in AOC compared with control (Fig. 7b; Table S6).

Discussion

The results of the *in planta* oviposition Expt I generally confirmed previous results from *in vitro* experiments that tested the effects of SC on the performance of weevil larvae (Whitehill *et al.*, 2016b). It was surprising, at first, that larvae in Expt II also performed more poorly on R trees than on S trees, although trees were inoculated below the SC-rich area of the apical shoot tip. In Expt II, larvae on both the R and the S trees were exposed to flooding of galleries by oleoresin, suggesting that in this scenario oleoresin acted as the major defense, and differences in larval performance may be attributed to the difference in oleoresin composition between the R and S trees. As observed here and previously reported (Robert *et al.*, 2010; Hall *et al.*, 2011), the R trees contained higher amounts of (+)-3-carene and dehydroabietic acid, which were associated with weevil resistance (Robert *et al.*, 2010). Flooding of galleries also occurred on R trees in Expt I, suggesting that if oviposition occurs on R trees in nature, SC and oleoresin act synergistically. Stone cells appear to hinder establishment of neonate larvae and slow larval development, even in the absence of oleoresin, as documented with feeding experiments on artificial diet (Whitehill *et al.*, 2016b). *In planta*, the slower developing larvae on R trees will be exposed to

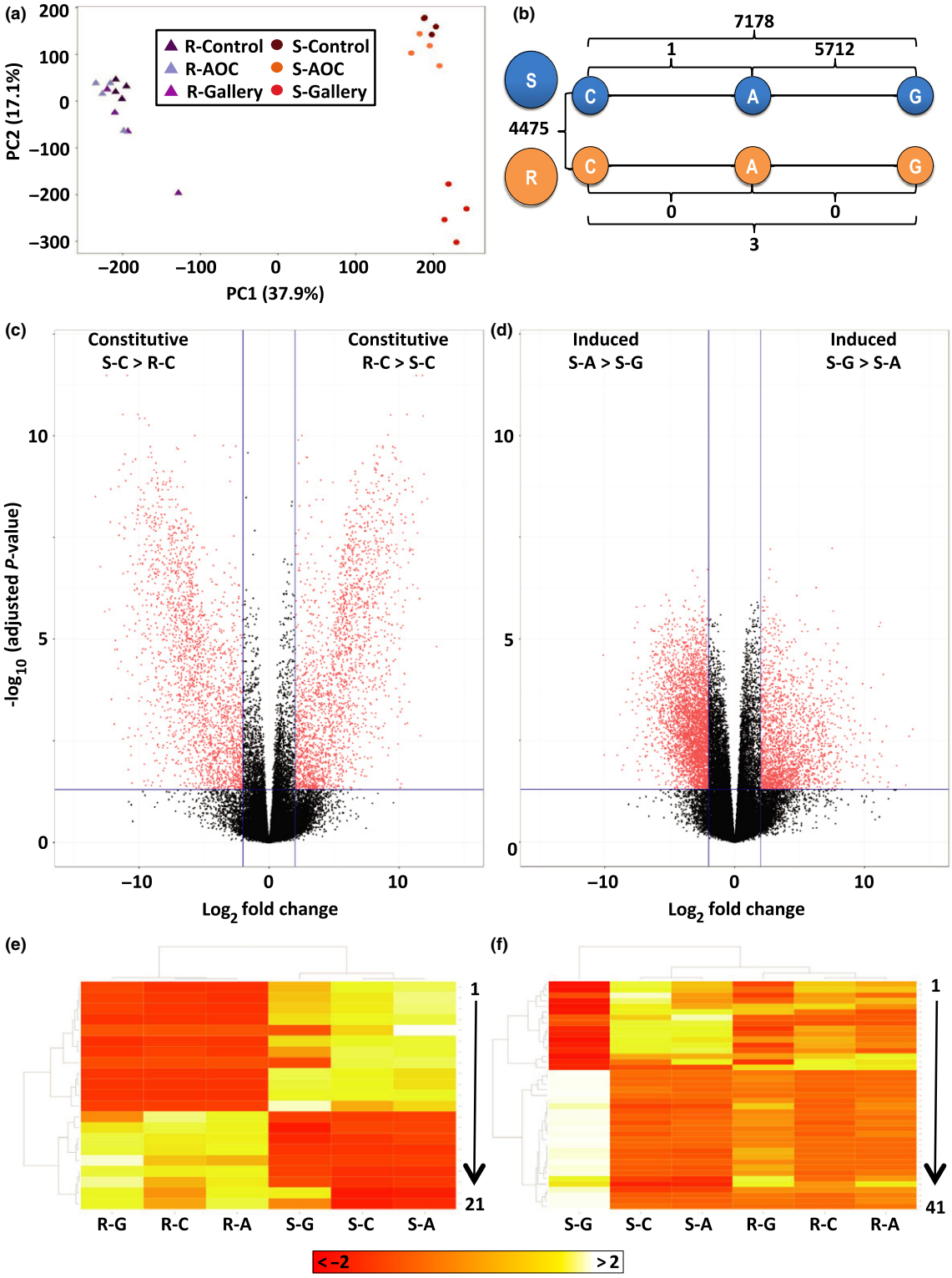

Fig. 7 Long-term treatment effects on resistant (R) and susceptible (S) trees transcriptome in Expt I mimicking natural oviposition and larval development. (a) Principal component analysis (PCA) of Sitka spruce cortex transcriptomes. Each color point represents a single biological replicate from the R (triangles) and S (circles) trees. AOC, artificial oviposition chamber. (b) Overall number of differentially expressed (log_2-fold change > 2; $P \leq 0.05$) contigs (i.e. transcripts) between R and S from untreated controls (C), artificial oviposition chambers (A), and weevil gallery (G) tissues. (c) Volcano plot of differentially expressed contigs for constitutive differences between R and S trees. (d) Volcano plot of differentially expressed contigs for the long-term induced response of S trees to active weevil feeding. Heatmaps of known conifer defense genes from constitutive (e) differences between genotypes and the long-term induction response (f) of S Sitka spruce. Heatmaps were generated from cpms of all four biological replicates averaged for each treatment × genotype combination. Overall expression levels were scaled within row to between −2 and +2 for each individual gene. Genes with higher relative expression levels are shown in yellow, and genes with lower relative expression levels are shown in red. White cells in heatmaps represent a relative expression level > +2.

potentially more toxic or otherwise more inhibitory composition of oleoresin, being both trapped and poisoned. In contrast, on the S trees larvae do not have to contend with a high abundance of SC and were apparently not affected to the same degree by volume and composition of oleoresin in Expt I. Frass from larvae that experienced oleoresin flooding showed monoterpene and diterpene concentrations that exceeded the concentration in the phloem tissue. The higher levels of terpenes in the frass may be due to accumulation of undigested terpenes as they pass through the insect's digestive system and become enriched in the frass. It is also possible that terpenes are being absorbed into frass after excretion. Larvae in Expt II did not reach the SC zone on the R trees, despite their unexpected and unusual acropetal gallery formation. It is not clear what caused the acropetal movement of weevils in Expt II. It may be directed by the larvae searching for nutrients that are less abundant or accessible at the lower positions of the PYAS. Curiously, larvae in Expt II moved towards the location where they would have hatched if left to the natural oviposition behavior of the adult female.

Differences between larvae from R and S spruce in Expts I and II support the hypothesis that fortifying the top of the PYAS tip with SC is an effective strategy against insect feeding. Mandible wear was visible in the two larvae on R trees that had not progressed past the SC zone and had not developed beyond the 1st instar, but this observation can only be considered preliminary given the small sample size. While larvae arrested within the 1st instar had substantial mandible wear, larvae that passed the SC zone and progressed into the 3rd instar showed no visible signs of mandible damage. These results are consistent with observations of weevil larvae on artificial diet containing SC (Whitehill *et al.*, 2016b). Stone cells appear to affect mandibles, but renewal of mandibles when larvae molt into advanced instars may allow them to overcome the damage caused by SC on mandibles. We therefore conclude that mandible wear is not the main mode of operation for SC, but that their effect on the nutritional quality of the phloem may be more important (Whitehill *et al.*, 2016b).

Larvae that had fed on R trees showed effects on gut bacteriomes, confirming observations from *in vitro* feeding assays on SC-enriched artificial diets (Whitehill *et al.*, 2016b). In other conifer-feeding weevil species, the gut microbiome has recently been shown to be important for the insect to deal with host chemical defenses such as terpenes (Berasatequi *et al.*, 2016, 2017). In the Sitka spruce interaction with spruce weevil larvae, it is not clear if the affected bacteriomes are merely a consequence of overall reduced weevil performance, or if the lesser developed bacteriomes affect the weevils' abilities to cope with host defenses such as terpenes as shown in other weevils (Berasatequi *et al.*, 2016, 2017). Future work will explore this question following the elegant approaches of Berasatequi *et al.* (2016, 2017) in their study of the composition and functions of weevil gut microbiomes. Specifically, it will be interesting to test if the microbial content of a healthy bacteriome would allow the spruce weevil to cope with (+)-3-carene and dehydroabietic acid which it encounters on the R trees.

Resistant and susceptible trees also showed strikingly different transcriptome responses at the 50-d time point after oviposition. Previous work focused on short-term induced transcript induction within hours or days of real or simulated adult weevil attack (Miller *et al.*, 2005; Ralph *et al.*, 2006, 2008), but did not examine the long-term response to sustained larval feeding. At the 50-d time point, only S trees had sustained a strong signature of a DE transcriptome. It is important to note that the apparent lack of a DE transcriptome in the R trees at the late time point does not exclude a transcriptome response at an earlier time point. The observed differences in the transcriptome responses may be due to tree genotype, or may be explained by the higher activity of weevil feeding in S trees compared with R trees. The DE transcriptome includes signatures of phenolic and terpenoid defense metabolism.

Stone cells as a durable defense of conifers have received considerable attention in Sitka spruce and Norway spruce (Wainhouse *et al.*, 1990; King *et al.*, 2011). In addition to the Sitka spruce – *Pissodes* weevil system, Sitka spruce and Norway spruce with a high abundance of SC in the bark had reduced larvae survival and were less attacked by great spruce bark beetle (*Dendroctonus micans*) adults (Wainhouse *et al.*, 1990). Bark beetles of the genus *Dendroctonus* attack members of the Pinaceae worldwide and are among the most devastating pests economically and ecologically to North American forest ecosystems (Vega & Hofstetter, 2015). The work by King *et al.* (2011) and Wainhouse *et al.* (1990) suggests that SC are an important trait to select for in conifer breeding for resistance. It is not known if SC, and SC interactions with oleoresin terpenes, also contribute to defense in other conifer herbivore interactions, such as defense of pine and spruce seedlings against *Hylobius* weevils. Variation of susceptibility against *Hylobius abietis* is attributed to the composition and quantity of oleoresin terpenes (Zas *et al.*, 2005). Future research into SC in this and other conifer pest interactions is warranted, and exploring the genetic underpinnings of SC may enable the breeding of conifers with enhanced resistance against various stem-feeding insects.

We had previously proposed that SC function in conifer defense against insects through several mechanisms (Whitehill *et al.*, 2016b) that include: (1) acting as a physical barrier that prevent establishment and movement of neonate larvae; (2) possibly mandible damage to neonate and early instar larvae that may impact feeding; and (3) physical displacement of nutritious host tissue. These physical defenses cannot easily be overcome. In addition, the physical constraint caused by SC, which slows development and movement of weevil larvae through the cortex, is likely to enhance the impacts of oleoresin terpenes by longer exposure of smaller and less well developed larvae. The combination of SC and oleoresin terpenes represents a synergistic 'conifer defense syndrome' that functions as a robust defense against spruce weevil. According to Agrawal & Fishbein (2006), defense syndromes are comprised of several defensive traits that minimize herbivory. Curiously, SC defenses that are formed in the spruce cortex and act against weevils (Whitehill *et al.*, 2016a,b) resemble sand-based defenses on the surfaces of sticky plants that entrap sand with glandular trichomes, which fends off herbivory through a combination of mechanisms that may include mandible wear and anti-nutritive effects (Lopresti & Karban, 2016; Lopresti *et al.*, 2018). These similarities suggest that

different plant species have evolved, or coopted, different strategies to arrive at the same effect of fortifying vulnerable tissues with sand or sand-like structures such as SC as a durable physical defense against herbivores.

Acknowledgements

We thank members of the Bohlmann laboratory for assistance: Carol Ritland for project management; Angela Chiang, Elizabeth Steves and Callum Kingwell for technical assistance. We thank Garnet Martens, Kevin Hodgson, Derrick Horne, and Bradford Ross for technical support at the University of British Columbia Bioimaging Facility. We thank Ward Strong at the BC Ministry of Forests, Lands, and Natural Resource Operations for discussion. We also thank the three anonymous reviewers for their very insightful comments and suggestions. The work was supported with funds from Genome Quebec, Genome BC, and Genome Canada to JB for the SpruceUp Project, and funds from the Natural Sciences and Engineering Research Council (NSERC) of Canada Discovery Grant to JB. JB is a UBC Distinguished University Scholar.

Author contributions

JGAW and J. Bohlmann planned and designed the research. JGAW, HH, LM, and KK performed experiments. BJ provided insects and guidance with weevil biology. MMSY and J Bryan provided RNA-seq analysis pipelines. JGAW and MMSY analyzed data. JGAW and J Bohlmann interpreted the results and wrote the manuscript. All authors reviewed and edited the manuscript.

ORCID

Jörg Bohlmann http://orcid.org/0000-0002-3637-7956
Jennifer Bryan http://orcid.org/0000-0002-6983-2759
Lina Madilao http://orcid.org/0000-0003-4161-2540
Justin G. A. Whitehill http://orcid.org/0000-0003-2578-9522
Macaire M. S. Yuen http://orcid.org/0000-0003-3179-6956

References

Agrawal AA, Fishbein M. 2006. Plant defense syndromes. *Ecology* **87**: 132–149.

Alfaro RI, Borden JH, King JN, Tomlin ES, McIntosh RL, Bohlmann J. 2002. Mechanisms of resistance in conifers against shoot infesting insects: the case of the white pine weevil *Pissodes strobi* (Peck) (Coleoptera: Curculionidae). In: Wagner MR, Clancy KM, Lieutier F, Paine TD, eds. *Mechanisms and deployment of resistance in trees to insects*. the Netherlands: Klubbert Publ, 101–126.

Andrews S. 2010. FastQC: a quality control tool for high throughput sequence data. [WWW document] URL http://www.bioinformatics.babraham.ac.uk/projects/fastqc.

Berasategui A, Axelsson K, Nordlander G, Schmidt A, Borg-Karlson AK, Gershenzon J, Terenius O, Kaltenpoth M. 2016. The gut microbiota of the pine weevil is similar across Europe and resembles that of other conifer-feeding beetles. *Molecular Ecology* **25**: 4014–4031.

Berasategui A, Salem H, Paetz C, Santoro M, Gershenzon J, Kaltenpoth M, Schmidt A. 2017. Gut microbiota of the pine weevil degrades conifer diterpenes and increases insect fitness. *Molecular Ecology* **26**: 4099–4110.

Bolger AM, Lohse M, Usadel B. 2014. Trimmomatic: a flexible trimmer for Illumina sequence data. *Bioinformatics* **30**: 2114–2120.

Bushnell B. 2017. BBMap short read aligner, and other bioinformatic tools. [WWW document] URL http://sourceforge.net/projects/bbmap/.

Celedon JM, Yuen MMS, Chiang A, Henderson H, Reid KE, Bohlmann J. 2017. Cell-type- and tissue-specific transcriptomes of the white spruce (*Picea glauca*) bark unmask fine-scale spatial patterns of constitutive and induced conifer defense. *Plant Journal* **92**: 710–726.

Cheng J. 2016. Interactive Heat Maps Using 'htmlwidgets' and 'D3.js'. [WWW document] URL https://cran.r-project.org/web/packages/d3heatmap/.

Franceschi VR, Krokene P, Christiansen E, Krekling T. 2005. Anatomical and chemical defenses of conifer bark against bark beetles and other pests. *New Phytologist* **167**: 353–376.

Franceschi VR, Krokene P, Krekling T, Christiansen E. 2000. Phloem parenchyma cells are involved in local and distant defense responses to fungal inoculation or bark-beetle attack in Norway spruce (Pinaceae). *American Journal of Botany* **87**: 314–326.

Fu L, Niu B, Zhu Z, Wu S, Li W. 2012. CD-HIT: accelerated for clustering the next generation sequencing data. *Bioinformatics* **28**: 3150–3152.

Grabherr MG, Haas BJ, Yassour M, Levin JZ, Thompson DA, Amit I, Adiconis X, Fan L, Raychowdhury R, Zeng Q *et al.* 2011. Full-length transcriptome assembly from RNA-seq data without a reference genome. *Nature Biotechnology* **29**: 644–652.

Haas BJ, Papanicolaou A, Yassour M, Grabherr M, Blood PD, Bowden J, Couger MB, Eccles D, Li B, Lieber M *et al.* 2013. *De novo* transcript sequence reconstruction from RNA-Seq: reference generation and analysis with Trinity. *Nature Protocols* **8**: 1494–1512.

Hall DE, Robert JA, Keeling CI, Domanski D, Quesada AL, Jancsik S, Kuzyk MA, Hamberger B, Borchers CH, Bohlmann J. 2011. An integrated genomic, proteomic and biochemical analysis of (+)-3-carene biosynthesis in Sitka spruce (*Picea sitchensis*) genotypes that are resistant or susceptible to white pine weevil. *Plant Journal* **65**: 936–948.

Hamberger B, Ohnishi T, Hamberger B, Séguin A, Bohlmann J. 2011. Evolution of diterpene metabolism: Sitka spruce CYP720B4 catalyzes multiple oxidations in resin acid biosynthesis of conifer defense against insects. *Plant Physiology* **157**: 1677–1695.

Hammerbacher A, Paetz C, Wright LP, Fischer TC, Bohlmann J, Davis AJ, Fenning TM, Gershenzon J, Schmidt A. 2014. Flavan-3-ols in Norway spruce: biosynthesis, accumulation, and function in response to attack by the bark beetle-associated fungus *Ceratocystis polonica*. *Plant Physiology* **164**: 2107–2122.

Keeling CI, Bohlmann J. 2006. Diterpene resin acids in conifers. *Phytochemistry* **67**: 2415–2423.

King JN, Alfaro RI. 2009. *Developing Sitka spruce populations for resistance to the white pine weevil: summary of research and breeding program*. Victoria, BC, Canada: B. C. Ministry of Forests and Range.

King JN, Alfaro RI, Lopez MG, Akker LV. 2011. Resistance of Sitka spruce (*Picea sitchensis* (Bong.) Carr.) to white pine weevil (*Pissodes strobi* Peck): characterizing the bark defence mechanisms of resistant populations. *Forestry* **84**: 83–91.

Kiss GK, Yanchuk AD. 1991. Preliminary evaluation of genetic variation of weevil resistance in interior spruce in British Columbia. *Canadian Journal of Forest Research* **21**: 230–234.

Kolosova N, Bohlmann J. 2012. Conifer defense against insects and fungal pathogens. In: Matyssek R, ed. *Growth and defence in plants: resource allocation at multiple scales*. Berlin, Germany: Springer-Verlag, vol. **220**, 85–109.

Law CW, Chen Y, Shi W, Smyth GK. 2014. Voom: precision weights unlock linear model analysis tools for RNA-seq read counts. *Genome Biology* **15**: R29.

Lopresti E, Grof-Tisza P, Robinson M, Godfrey J, Karban R. 2018. Entrapped sand as a plant defense: effects on herbivore performance and preference. *Ecological Entomology* **43**: 154–161.

Lopresti E, Karban R. 2016. Chewing sandpaper: grit, plant apparency, and plant defense in sand-entrapping plants. *Ecology* **97**: 826–833.

Mageroy M, Lachance D, Jancsik S, Parent G, Séguin A, Mackay J, Bohlmann J. 2017. *In vivo* function of Pgβglu-1 in the release of acetophenones in white spruce. *Peer J* **5**: e3535.

Martin DM, Tholl D, Gershenzon J, Bohlmann J. 2002. Methyl jasmonate induces traumatic resin ducts, terpenoid resin biosynthesis, and terpenoid accumulation in developing xylem of Norway spruce stems. *Plant Physiology* **132**: 1586–1599.

Miller B, Madilao LL, Ralph S, Bohlmann J. 2005. Insect-induced conifer defense. White pine weevil and methyl jasmonate induce traumatic resinosis, *de novo* formed volatile emissions, and accumulation of terpenoid synthase and putative octadecanoid pathway transcripts in Sitka spruce. *Plant Physiology* **137**: 369–382.

Nagel R, Berasategui A, Paetz C, Gershenzon J, Schmidt A. 2014. Overexpression of an isoprenyl diphosphate synthase in spruce leads to unexpected terpene diversion products that function in plant defense. *Plant Physiology* **164**: 555–569.

Patro R, Mount SM, Kingsford C. 2014. Sailfish enables alignment-free isoform quantification from RNA-seq reads using lightweight algorithms. *Nature Biotechnology* **32**: 462–464.

R Core Team. 2013. *R: a language and environment for statistical computing.* Vienna, Austria: R Foundation for Statistical Computing. [WWW document] URL: http://www.R-project.org/.

Raffa KF. 2014. Terpenes tell different tales at different scales: glimpses into the chemical ecology of conifer-bark beetle-microbial interactions. *Journal of Chemical Ecology* **40**: 1–20.

Ralph SG, Chun HJE, Kolosova N, Cooper D, Oddy C, Ritland CE, Kirkpatrick R, Moore R, Barber S, Holt RA *et al.* 2008. A conifer genomics resource of 200,000 spruce (*Picea* spp.) ESTs and 6,464 high-quality, sequence-finished full-length cDNAs for Sitka spruce (*Picea sitchensis*). *BMC Genomics* **9**: 484.

Ralph SG, Yueh H, Friedmann M, Aeschliman D, Zeznik JA, Nelson CC, Butterfield YSN, Kirkpatrick R, Liu J, Jones SJM *et al.* 2006. Conifer defence against insects: microarray gene expression profiling of Sitka spruce (*Picea sitchensis*) induced by mechanical wounding or feeding by spruce budworms (*Choristoneura occidentalis*) or white pine weevils (*Pissodes strobi*) reveals large-scale changes of the host transcriptome. *Plant Cell & Environment* **29**: 1545–1570.

Roach CR, Hall DE, Zerbe P, Bohlmann J. 2014. Plasticity and evolution of (+)-3-carene synthase and (-)-sabinene synthase functions of a Sitka spruce monoterpene synthase gene family associated with weevil resistance. *Journal of Biological Chemistry* **289**: 23859–23869.

Robert JA, Bohlmann J. 2010. Behavioral and reproductive response of white pine weevil (*Pissodes strobi*) to resistant and susceptible Sitka Spruce (*Picea sitchensis*). *Insects* **1**: 3–19.

Robert JA, Madilao LL, White R, Yanchuk A, King J, Bohlmann J. 2010. Terpenoid metabolite profiling in Sitka spruce identifies association of dehydroabietic acid, (+)-3-carene, and terpinolene with resistance against white pine weevil. *Botany-Botanique* **88**: 810–820.

Vega FE, Hofstetter RW. 2015. *Bark beetles: biology and ecology of native and invasive species.* London, UK: Academic Press.

Wainhouse D, Cross DJ, Howell RS. 1990. The role of lignin as a defense against the Spruce Bark Beetle *Dendroctonus micans* – effect on larvae and adults. *Oecologia* **85**: 257–265.

Warren RL, Keeling CI, Yuen MMS, Raymond A, Taylor GA, Vandervalk BP, Bohlmann J. 2015. Improved white spruce (*Picea glauca*) genome assemblies and annotation of large gene families of conifer terpenoid and phenolic defense metabolism. *Plant Journal* **83**: 189–212.

Whitehill JGA, Henderson H, Schuetz M, Skyba O, Yuen MMS, King J, Samuels AL, Mansfield SD, Bohlmann J. 2016a. Histology and cell wall biochemistry of stone cells in the physical defence of conifers against insects. *Plant, Cell & Environment* **39**: 1646–1661.

Whitehill JGA, Henderson H, Strong W, Jaquish B, Bohlmann J. 2016b. Function of Sitka spruce stone cells as a physical defense against white pine weevil. *Plant, Cell & Environment* **39**: 2545–2556.

Zas R, Sampedro L, Prada E, Fernández-Lopez J. 2005. Genetic variation of *Pinus pinaster* Ait. seedlings in susceptibility to the pine weevil *Hylobius abietis* L. *Annals of Forestry Science* **62**: 681–688.

Zulak KG, Dullat HK, Keeling CI, Lippert D, Bohlmann J. 2010. Immunofluorescence localization of levopimaradiene/abietadiene synthase in methyl jasmonate treated stems of Sitka spruce (*Picea sitchensis*) shows activation of diterpenoid biosynthesis in cortical and developing traumatic resin ducts. *Phytochemistry* **71**: 1695–1699.

Supporting Information

Additional Supporting Information may be found online in the Supporting Information section at the end of the article:

Fig. S1 Histology of weevil larval frass from R and S trees.

Fig. S2 Scanning electron microscopy images of weevil larvae bacteriomes.

Fig. S3 Metabolite profiles of different monoterpenes detected in Expts I and II in R and S tree cortex.

Fig. S4 Metabolite profiles of four monoterpenes only detected in R and S tree cortex from Expt II.

Fig. S5 Interactive heatmap of differentially expressed contigs with known conifer defense gene annotations identified from constitutive differences between R and S trees.

Fig. S6 Interactive heatmap of differentially expressed contigs with known conifer defense gene annotations identified from long-term induced responses of S tissues to weevil larvae feeding.

Methods S1 Expt II methods describing rearing of neonate weevils on semi-artificial diets with and without antibiotics, complete histology methods, and detailed methodology relating to the analysis of monoterpenes and diterpenes.

Table S1 Metabolite profiles of diterpene olefins, alcohols, aldehydes, and acids in weevil R and S Sitka spruce bark in Expt I.

Table S2 Metabolite profiles of diterpene olefins, alcohols, aldehydes, and acids in weevil R and S Sitka spruce bark in Expt II.

Table S3 RNA-seq transcriptome assembly statistics.

Table S4 Complete list of DE genes from constitutive differences between R and S Sitka spruce control tissues.

Table S5 Complete list of DE known conifer defense genes from constitutive differences between R and S Sitka spruce control tissues.

Table S6 Complete list of DE genes from larvae gallery induced feeding vs untreated control tissues on R trees.

Table S7 Complete list of DE genes from larvae gallery induced feeding vs untreated control tissues on S trees.

Table S8 Complete list of DE genes from larvae gallery induced feeding vs AOC tissues on S trees.

Table S9 Complete list of DE known conifer defense genes from long-term induced feeding differences between S Sitka spruce insect fed and AOC tissues.

Table S10 Complete list of DE genes from artificial oviposition chambers induced differences (S AOC vs S control) of S Sitka spruce.

Please note: Wiley Blackwell are not responsible for the content or functionality of any Supporting Information supplied by the authors. Any queries (other than missing material) should be directed to the *New Phytologist* Central Office.